IOP Publishing
Journal Title
Journal **XX** (XXXX) XXXXXX
https://doi.org/XXXX/XXXX

Halide Perovskites: Current Issues and New Strategies to Push Material and Device Stability

Giorgio Schileo[1], Giulia Grancini[1]

[1] Department of Chemistry, University of Pavia, Via Taramelli 14, 27100 Pavia, Italy

E-mail: giulia.grancini@unipv.it

Received xxxxxx
Accepted for publication xxxxxx
Published xxxxxx

Abstract

This short review aims at summarising the current challenges related to poor Perovskite Solar Cells (PSCs) stability which nowadays puts severe constrains on near future device commercialization. As a game changer in the field of photovoltaics (PVs), PSCs are highly efficient and cheap to fabricate. However, they suffer from poor long-term stability upon exposure to heat, moisture, oxygen and light, and combinations thereof. Poor device stability originates from intrinsic instability issues of the perovskite active layer itself, as well as extrinsic factors due to partial degradation of the layers composing the device stack. Here we briefly review the chemical and physical processes responsible for intrinsic material instability, and we highlight possible solutions to overcome it; we then consider the whole device, discussing properties and interactions of the stacked layers. Finally, particular emphasis is placed on the need of shared standards for stability tests, which should include detailed report on experimental conditions over a statistically significant number of samples, allowing for a direct comparison of results across different groups and fostering a rapid advance of our understanding of degradation mechanisms and of the solutions to overcome them.

Keywords: Perovskite; solar cell; photovoltaics; long term stability; degradation; 2D; scale-up.

1. Introduction

After merely a decade since their first application in photovoltaics (PVs)[1], organic-inorganic halide perovskites solar cells have now demonstrated power conversion efficiencies (PCE) beyond 25% by using inexpensive materials and cheap fabrication processes. However, the PV community involved in the development of this potentially disruptive technology is now facing a big issue which prevents Perovskite Solar Cells (PSCs) from entering the market: their short stability along with the need to improve the device performances over large area.

Since the first inorganic perovskite, $CaTiO_3$, was discovered in 1839, all minerals with the same ABO_3 structure, where A and B and metal cations, fall in the perovskites category. The larger A cation sits in the 12-fold coordinated site formed by $[BO_6]^{2-}$ corner-sharing octahedra (B is usually a +4 cation).

The Goldschmidt tolerance factor, expressed as

$$\tau = \frac{r_A + r_O}{\sqrt{2}(r_B + r_O)},$$

where r_A and r_B are the ionic radii of the A and B cation and r_O is the radius of oxygen, is a useful tool that has been used to predict the stability of inorganic perovskites. It is purely based on geometrical considerations: if

$$0.8 \leq \tau \leq 1$$

the perovskite structure is stable.

Hybrid organic-inorganic halide perovskites also possess the general formula ABX_3, where A is an organic cation (typically an alkylammonium ion), B represents Pb^{2+}, Sn^{2+}, Ge^{2+} or other divalent metals, and X is a halogen (F^-, Cl^-, Br^-, I^-) or pseudo-halogen (CN^-, BH_4^-). Methylammonium lead triiodide ($MAPbI_3$) is the prototypical halide perovskite. In this case, a tolerance factor of 0.912 applies, leading to a stable perovskite structure which cristallizes at room temperature in the tetragonal phase. Hybrid perovskites combine unique electrical and optical properties: high absorption coefficient, direct photo-generation of free carriers, efficient charge transport and long carrier diffusion lengths and wide band gap tunability, achieved by the manipulation of the A cation or the X halide. Another striking attribute of these materials is their low non-radiative recombination rates compared to other thin-film polycrystalline semiconductors[2–6]. PSCs can be fabricated in different configurations (Fig. 1). In general, the solar cell consists of a multi-layered structure where the perovskite is deposited between an *n*-type electron transport material (ETM), and a *p*-type hole transport material (HTM). The order and the nature of the layers determine the configuration of the cell. Inspired by the already established Dye Sensitized Solar Cells (DSSC), so-called mesoscopic PSCs consist of a compact layer of TiO_2 deposited on conductive fluorine-doped SnO_2/glass substrates, followed by a thicker layer of mesoporous TiO_2 nanoparticles. The perovskite infiltrates this mesoporous titania scaffold and also forms a capping layer, on top of which the HTM is deposited, typically an organic hole conductore such as Li-doped SPIRO-OMeTAD. Au contacts are evaporated to complete the circuit. Snaith and coworkers[7] found that PSCs can work also with a porous alumina scaffold, or even with no scaffold at all. The latter type is referred to as planar *n-i-p* structure. Alternatively, the opposite arrangement is also possible, where a *p*-type HTM such as the conductive poly(3,4-ethylenedioxythiophene) polystyrene sulfonate (PEDOT: PSS) is deposited first, followed by the perovskite and an ETM. In this case the most common choice for ETM is Phenyl-C_{61}-Butyric acid Methyl ester (PCBM). Au, Ag, Cu or Al can all be used as top metal contacts.

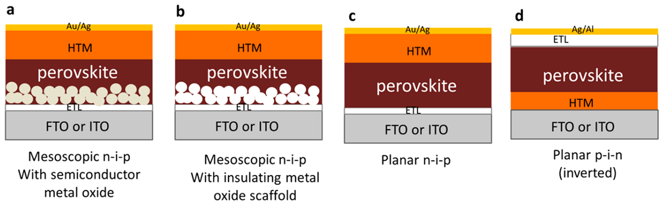

Mesoscopic n-i-p With semiconductor metal oxide

Mesoscopic n-i-p With insulating metal oxide scaffold

Planar n-i-p

Planar p-i-n (inverted)

Figure 1*. Main configurations for PSCs stacks. Reprinted (adapted) with permission from Chem. Rev.2019, 119, 5, 3036-3103. Copyright © 2019 American Chemical Society.*

2. Intrinsic Instability Factors

Despite the great potential as PV material in terms of power conversion efficiency, the instability of the perovskite solar cells is one of the main hindrances for larger scale applications. In particular, the prototypical hybrid perovskites have revealed inherently unstability. Poor stability is due to several concomitant factors derived from exposure to water, heat, oxygen, light and combination thereof. Here below we list a few of them, highlighting the degradation mechanism induced and the consequent effects on device stability.

2.1. Water

Prolonged exposure to water vapour triggers an irreversible material degradation which ultimately leads to conversion of the perovskite back to the initial precursors (such as PbI_2). More in detail, water forms hydrate complexes such as $(CH_3NH_3)_4PbI_6{\cdot}2H_2O$ and leaves out PbI_2, which tend to crystallize, driving the reaction forward. In addition, MA^+ is slightly acidic and reacts with water to form volatile methylamine and hydroiodic acid[8,9] according to the following reaction (1):

$$(CH_3NH_3)4PbI_6 \times 2H_2O \rightarrow PbI_2 + 4CH_3NH_3 + 4HI + 2H_2O \tag{1}$$

The reaction is not completely reversible because the products include volatile compounds (HI), but even in encapsulated devices solid PbI_2 and CH_3NH_3I tend to form locally isolated phases, so that they are no longer in contact and cannot re-form the perovskite[10].

2.2. Heat

$MAPbI_3$ is intrinsically unstable upon thermal stress which induces a release of I_2 and the appeareance of metallic Pb already at 40 °C (close to device working conditions) in the dark[11]. This is caused by the decomposition reactions (2) and (3):

$$CH_3NH_3PbI_3 \rightarrow CH_3NH_3I + PbI_2 \tag{2}$$

$$PbI_2 \rightarrow PbO(s) + I_2(g) \tag{3}$$

Even though reaction (3) is reversible (providing that I_2 does not escape the film or does not react with the metallic contacts), at just 80-85 °C methylammonium iodide disintegrates into more volatile compounds such as[12,13]:

$$CH_3NH_3I \rightarrow CH_3I + NH_3 \tag{4}$$

$$CH_3NH_3I \rightarrow CH_3NH_2 + HI \tag{5}$$

Both reactions are possible: (4) is thermodynamically more favoured, ~13-14 kcal mol^{-1} lower than (5), but it also requires a higher activation energy than (5) because of the higher number of bonds to break from the solid to the gas phase. Therefore, in the vast majority of cases, the observed decomposition products are CH_3NH_2 and HI[14]. The energy of formation of $MAPbI_3$, $MAPbBr_3$ and $MAPbCl_3$ has been calculated from Density Functional Theory (DFT) to be -0.1, -0.25 and -0.7 eV per unit cell, respectively. These values mean that the enthalpy gain is low compared to the precursors, and thus the opposite reaction (decomposition) can be triggered by a moderate increase in temperature[15]. Given that standard encapsulation procedures usually require exposing the cells at temperatures up to 160 °C, and that solar panels in the field routinely reach 65 °C or even ~80 °C at low latitudes, PSC are naturally exposed to thermal stress which must be controlled. A possible way to overcome the presented issue is to (partially) replace the MA with more thermally stable cations. Formamidinium (FA^+, $CH_3(NH_2)_2^+$) and cesium (Cs^+) are the most common A site substituents showing enhanced thermal stability. Compared to MA^+ (r_{MA+} = 217 pm), FA^+ is larger (r_{FA+} = 253 pm) and Cs^+ smaller (r_{Cs} = 188 pm) so that the structure deviates from a perfect perovskite (the tolerance factor τ is 0.85 and 0.99, respectively): in fact, $FAPbI_3$ crystallizes in the perovskite, black α-phase only above 165 °C. Below this temperature, even if quenched, it transforms into a yellow, non-photoactive δ-phase with hexagonal structure. Likewise, $CsPbI_3$ is stable at room temperature as a yellow orthorhombic δ-phase with an unsuitable bandgap of 2.7 eV, and possesses a suitable photoactive phase only above 315 °C. However, by mixing FA^+ and Cs^+ cations on the A site, the black α-phase can be stabilized at room temperature[16]. This has opened the way to more thermally stable hybrid perovskites, using for instance Cs^+ which is less volatile than MA^+, and cations like formamidinium or guanidinium (Gua^+, $CH_6N_3^+$) which are less acidic and can form more hydrogen bonds with the halogen increasing the structural robustness upon heating[17]. Partially substituting Br at the X site also improves stability, since Br^- is smaller than I^- leading to a shrinkage of the lattice and a strengthening of the cation-halide bonding, as also shown by theoretical calculations[18]. Mixing Br and I also allow us to easily tune the bandgap, a desired feature for instance for tandem cells[19]. Despite the advantages of such compositional cation engineering, such mixture brings a new issue related to the formation of photoinduced halide segregation[20], which can affect charge dynamics and device behavior as explained more in detail in §3.

2.3. Oxygen and light

Perovskite films are also susceptible to a combination of oxygen and light. Several studies[21–23] have shown that oxygen can diffuse from the crystal grain boundaries composing the perovskite polycristalline film over a time scale of minutes (with an estimated diffusion coefficient $D = 10^{-7}$-10^{-9} cm^2 s^{-1}); molecular oxygen then acts as an electron scavenger forming the highly reactive superoxide species O_2^- at iodine vacancy sites (favoured by the fact that O_2^- and I^- have similar ionic radii). The superoxide then reacts with the photoexcited perovskite, which, for the case of $MAPbI_3$ leads to (6):

$$4CH_3NH_3\mathrm{Pb}I_3^* \ + \ O_2^- \rightarrow 4\mathrm{Pb}I_2 \ + \ 2H_2\mathrm{O} + 4CH_3NH_3 + 2I_2 \quad (6)$$

If charges can be extracted efficiently the reaction time with adsorbed oxygen can be minimized, limiting this effect. However, since even low levels of oxygen are extremely detrimental and no encapsulation can ensure a perfect barrier for 25 years, different perovskite compositions with higher oxygen tolerance and appropriate dopants should be employed. For example, $FAPbI_3$ is a better alternative to $MAPbI_3$, and $FA_{0.9}Cs_{0.1}PbI_3$ is even a better candidate. Again, the reason behind that is found in the shrinkage ability of the crystal lattice caused by Cs^+, which strengthens the FA-I hydrogen bonds making it more robust[24]. More recently, unencapsulated devices based on $(FA_{0.79}MA_{0.16}Cs_{0.05})_{0.97}Pb(I_{0.84}Br_{0.16})_{2.97}$ appeared as a valid strategy, showing to retain ~90% of their initial efficiency after 1000 hours under illumination, at room temperature[25]. Furthermore, complete substitution of MA^+ recently resulted in even enhanced stability: $FA_{0.83}Cs_{0.17}Pb(I_yBr_{1-y})_3$ perovskite mixed with *n*-butylammonium cations (a large cation which forms layered perovskite platelets, see §4) showed a t_{80} (the time required for a cell to decrease to 80% of its initial efficiency) of 1000 hours at 50-60 °C when unencapsulated, and almost 4000 hours with encapsulation.

As a strategy to improve material stability, small monovalent metals like K^+ and Rb^+ have also been incorporated into the PSCs active layer. Being too small to be inserted in the perovskite framework, it has been suggested that they can sit at the interstitial sites of the perovskite lattice, inhibiting iodine vacancies migration[26] (see §3). Discussion on this is still open: recent solid state NMR studies have proven that neither Rb^+ nor K^+ can enter the perovskite lattice[27]: they rather segregate into phases such as δ-$Cs_{0.5}Rb_{0.5}PbI_3$. On the other side, Li *et al*[28] showed that small cations such as Li^+ and Na^+ can migrate through the perovskite, possibly influencing the long term stability of the devices. Regardless of the mechanism, K^+ doping can also affect the crystallization, yielding larger grains, while improving carrier lifetimes[26]. Larger grain size are also beneficial if considering that degradation reactions and non-radiative recombination both originate at defect (or trap) sites which are mainly located at the grain boundaries. Reducing the boundary-to-bulk ratio will also reduce the density of gates for water and oxygen penetration, thus limiting the material degradation.

3. Ion migration and photoinduced phase segregation

PSCs suffer of hysteretic behaviour in the current-voltage characteristic, which depended on scan speed, temperature and nature of the interfaces[29]. The presence of mobile ions with relatively small activation energy (E_a) for migration has been indicated to be one of the main reason behind this anomalous phenomenon, excluding other possible causes such as ferroelectricity. Early studies of possible defects in $MAPbI_3$ found that I^- and MA^+ vacancies require an E_a of 0.58 and 0.84 eV, respectively, to move through the perovskite lattice[30].

Other works[31,32] found even lower activation energies (~0.1 and ~0.5 eV, and ~0.8 eV for Pb^{2+}). Subsequent studies provided solid evidence of MA^+[33] and iodide[34] migration (Figure 2). Despite the different values for E_a of each species, the general consensus is that I^- is the fastest migrating ion, capable of crossing a film of $MAPbI_3$ in 1 µs, too fast to be responsible for the observed hysteresis effects, which occurr on the timescale of 0.1 to 100 s, and for which the slower MA^+ and Pb_2^+ cations are likely responsible instead. In terms of migration channels, the values presented so far have been calculated for single crystals, where vacancies (Schottky defects) enable the migration of ions[30]. However for polycrystalline films, grain boundaries represent the main migration channel[32]. Ion migration is intimately related to poor material stability and affects the performance of PSCs, since mobile ions can accumulate at the absorber/charge transport layer interfaces, modifying the band alignment and the charge extraction mechanism. A strategy to prevent ion migration is therefore of extreme interest. In 2014 Shao *et al.*[35] showed that passivation of trap states at the surface and at grain boundaries with fullerenes eliminated the hysteresis and doubled the power conversion efficiency of $MAPbI_3$ solar cells, corroborating the hypothesis that ion migration passes mainly through these channels. In 2015, Gratia *et al.*[20] and Hoke *et al.*[36] reported on the formation of an additional photoluminescence (PL) peak for $0.2 < x < 1.0$ in $MAPb(Br_xI_{1-x})_3$ perovskite films, accompanied by a splitting of X-ray diffraction (XRD) peaks, which suggested the formation of two separate iodine-rich and bromine-rich phases under illumination. This so-called photoinduced halide segregation or "*Hoke effect*" is reversible within a few minutes, but it is only partially reversible over a few hours, which limits the open circuit voltage of the resulting devices [37]. The rates of formation and recovery depend strongly on the halide concentration: the higher the halide concentration (stoichiometric excess), the faster the rate of both processes (segregation and recovery in the dark). Photosegregation is therefore related to the concentration of halide vacancies and to the different affinity of Pb_2^+ towards I^- and Br^-: although several explanations have been proposed for this phenomenon, for example a difference in dark and photoirradiated formation energies, or in the potential excited state energy minima, a model that accounts for all experimental conditions has not been developed yet[38].

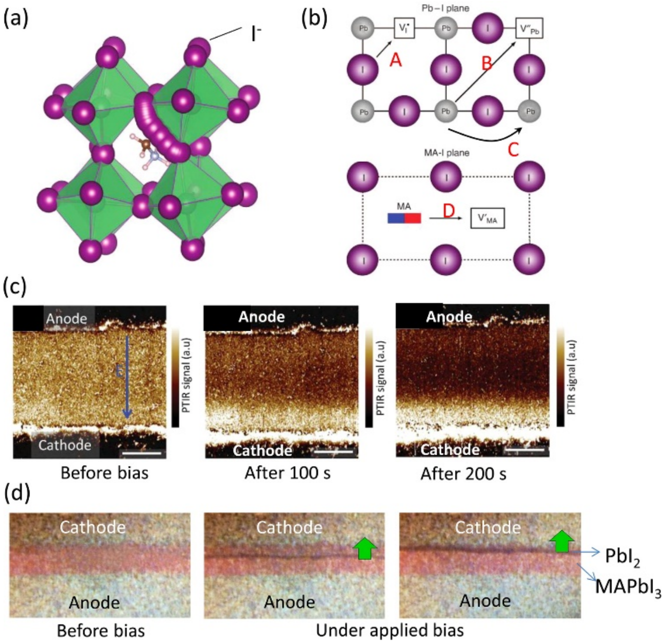

Figure 2*. (a) Migration path of I^- ions in $MAPbI_3$ calculated with DFT methods; (b Migration paths of I^-, Pb_2^+ and MA^+ ions used for the calculation of activation energies (E_a); (c) Photothermal Induced Resonance images showing the distribution of MA^+ ions before and after poling between two electrodes 100 µm apart; (d) Optical images of a PbI_2 thread (seen in cross section) in a $MAPbI_3$ perovskite solar cell which migrated along the applied electric field at 330 K. Reproduced with permission from Ref[32] .*

4. Low-Dimensional Perovskites

Recently, dimensionality tuning of the perovskite has attracted a great deal of attention, with a particular interest towards low-dimensional perovskites for their superior stability against moisture far above their standard three-dimensional parent structures. Layered perovskites usually possess the general structure $R_2A_{n-1}B_nX_{3n+1}$, where R is a large organic cation (for example, aliphatic or aromatic alkylammonium) which functions as a spacer between the inorganic sheet, and n determines the number of inorganic sheets that are being held together (see Fig. 3a). Controlling the A/R ratio, the n value could be adjusted from $n = 1$ (2D), $n > 1$ (quasi 2D), and $n = \infty$ (3D). For low n, 2D perovskites have large band gaps and stable excitons with large binding energy (as shown in the absorption spectra in Fig. 3b). Such properties are not ideal for photovoltaic action, therefore leading to poor performances in solar cells[39]. However, relative to 3D perovskites, 2D perovskites show remarkably higher moisture resistance. This greater stability is mainly due to the hydrophobic nature of the R cation, as well as the highly oriented structure and dense packing, which reduces the density of the grain boundaries and prevents direct contact of adventitious water with the perovskite[39]. The integration of 2D perovskites into PSCs as a stabilizer component has been recently proposed as a way to increase the lifetimes of PSCs. The aim of this approach is to combine the high efficiency of 3D perovskites with the superior stability of 2D perovskites, in a synergistic action. This has been demonstrated by either blending the 2D and 3D precursors toghether or by engineering a layer by layer deposition method to obtain a 2D/3D bilayer structure. The top 2D perovskite layers can simultaneously act as surface passivant, improving the surface robusteness and hydrophobic character of the active layer, while also reducing the surface charge recombination, ultimately improving the device open circuit voltage[40]. Cho *et al.*[41] developed a two-step method for the deposition of a 3D/2D bilayer composed of $MAPbI_3$ and PEI_2PbI_4[39]. The layer-by-layer growth is induced by dynamically spin coating PEAI in isopropanol solution on the mixed halide 3D perovskite with excess PbI_2. The excess PbI_2 has been demonstrated to segregate on the top of the 3D perovskite. The PEAI thus reacts in situ with the PbI_2 at the top surface, forming a thin layer of 2D on top of the 3D (see the model of the device architecture in Fig. 3c). As the 2D perovskite lies on the top surface at the interface with the HTM, interfacial charge-carrier recombination is reduced and the PCE increases to >20%, retained for 800 h at 50 °C under 1 Sun illumination in an ambient environment. Importantly, this result demonstrated that it is possible to achieve enhanced stability without compromising the PCE. The 2D perovskite can be also developed at the bottom surface of a *n-i-p* device architecture, anchoring on the TiO_2 surface. With this idea, a 2D/3D composite of $AVA_2PbI_4/MAPbI_3$ has been developed[42]. This composite was fabricated using a simple one-step deposition approach in which the precursor solutions were blended together. The -COOH end groups in AVA^+ anchor to the mesoporous TiO_2 layer, resulting in the formation of a thin 2D layer at the oxide surface. This induces a vertically graded structure, in which the 2D perovskite templates the growth of a highly oriented 3D perovskite film on top, forming a 2D/3D layered system. This layered 2D/3D architecture has been implemented in standard mesoporous TiO_2/SPIRO-OMeTAD solar cells as either a 3D/2D or 2D/3D active layer in an inverted configuration, and in monolithic solar cells in which the HTM and gold electrode are replaced by a carbon layer[42]. The latter configuration is of great interest owing to the lower cost of carbon and enhanced resistivity to water permeation, which makes it an intrinsically more stable configuration. In both the standard and inverted configuration, enhanced stability was obtained, which is ascribed to the greater structural stability of the 2D/3D layers as well as to possible passivation of the TiO_2 surface through the 2D perovskite bonds. In particular, for the monolithic devices (0.5 cm^2 laboratory-scale cells and 10 x 10 cm^2 large modules, see Fig. 3d), the 2D/3D composite approach achieved a world-record stability of more than one year. These devices showed no loss in performance over 10,000 h of testing (at 55 °C, 1 sun illumination for 24 h per day, sealed under ambient atmosphere). This work has triggered much academic and industrial interest and shows the potential for scaling up perovskite technologies[39].

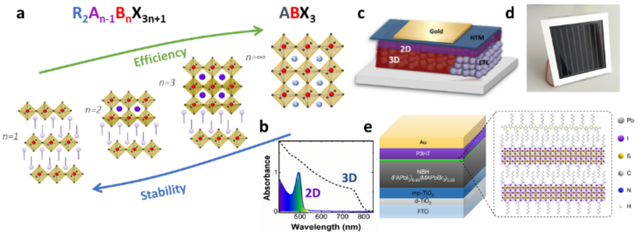

***Figure 3**. a. Structure of perovskite from 2D to 3D. b. Comparison of absorption spectra for a typical 2D (n=1) and 3D perovskite thin film. c. Schematics of n-i-p solar cell architecture using the 3D/2D bilayer as active material. d. Picture of the 10x10 cm module realized by Solaronix® based on monolithic solar cell using a mixture of 2D and 3D blend (courtesy of Solaronix®). e. Structure of an* n-i-p *perovskite solar cell based on a DHA using P3HT as the hole-transport material. FTO, fluorine-doped tin oxide; d-TiO_2, dense titanium dioxide; mp-TiO_2, mesoporous titanium dioxide. Right, schematic structure of the interface between the WBH and P3HT (adapted from Ref [43]).*

More recently, *Jung et al.* reported a double-layered halide architecture (DHA) using an ultrathin wide-bandgap halide (WBH) stacked onto a narrow-bandgap-halide light-absorbing layer, prior to deposition of the HTM (Fig. 3 e). Inserting the WBH layer effectively reduced charge recombination at the perovskite/P3HT interface. This resulted in PCE around 23% and long-term operational stability for 1,370 hours under 1-Sun illumination at room temperature, maintaining 95% of the initial efficiency[43].

5. Stability of other layers in the stack

The intrinsic stability of the extra materials needed to extract charges from the perovskite layer and their interplay with each other is crucial to the long-term stability of the whole device. Earliest high efficiency *n-i-p* mesoscopic PSCs were based on the glass/FTO/TiO_2/meso-TiO_2/$MAPbI_3$/SPIRO-OMeTAD/Au stack. Notably, Spiro-OMeTAD crystallizes at about 100 °C[44], and is permeable to iodine, which reduces it and decreases its conductivity. It also has to be doped with Li-TFSI (Lithium bis(trifluoromethane-sulfonyl)imide) to improve its hole conductivity, but Li-TFSI attracts water which in turns attacks the perovskite layer. Li^+ can also migrate through the perovskite[28]. Similarly, other organic HTMs such as P3HT (poly(-hexylthiophene)) or PTAA (Poly[bis(4-phenyl)(2,4,6-trimethylphenyl)amine]) are unlikely to survive 25 years of operation in the field, and besides are way too expensive for mass production. For these reasons, researchers have been looking at inorganic HTMs such as doped and undoped NiO_x[45–47], Cu_2O and CuO[48,49], CuI[50,51] and CuSCN[52,53], and obtained high efficiencies, albeit somewhat lower than with organic HTMs. For *p-i-n* configurations, inorganic ETL such as SnO_2 and ZnO have been proposed. Although they cannot further oxidize (except for NiO_x), metal oxides can however catalyze oxygen degradation of the materials with which they are in contact when exposed to UV light. In fact, TiO_2 is widely used as photocatalyst for water splitting and as coating for self-cleaning surfaces. Unless deactivated through an appropriate coating like CsBr[54], TiO_2 based PSCs are less stable than their SnO_2 counterparts, which survived for 1000 hours in presence of light, moisture and oxygen (at room temperature)[25]. New oxides have been also been also proposed to circunvent the issue related to TiO_2 catalytic effect. Among these, an interesting approach has been shown by *Lira-Cantu*'s group exploiting a thin film of $Pb[Zr_xTi_{1-x}]O_3$ (PZT) ferroelectric oxide as the ETM in planar configuration. The solar cells were poled up to 2 V in order to polarize the PZT electrode. Poling resulted in a slow but steady improvement of the photovoltaic properties of the PZT-based PSC. The improvement was observed during the first 90 minutes after which the device stabilized and then maintained its photovoltaic properties under continuous illumination in air for hours[55,56].

Back contacts usually consist of evaporated Au, Ag, Cu or Al layers: almost all metals react with halogens or halides or, like Au, migrates through the perovskite creating shunting paths[57,58]. While useful in assessing the efficiency of a particular composition, alternative solutions must be adopted for long term stability. Adding a barrier layer between the back contact and the HTM, such as MoO_x/Al_2O_3[25], Al-doped ZnO (AZO)/SnOx[59], ITO[60] or others[58] did not succeed in completely stopping the diffusion of species: stability studies are conducted either in the dark, or at low temperature, or for just a few hundred hours. The study by Park and coworkers[61] show PCE retained by 87% of its initial value after 500 h under 1 Sun illumination at 85 °C by placing an AZO barrier film by Atomic Layer Deposition (ALD) between the PCBM/BCP layer and the Ag or Al contact. Also ITO can be an effective barrier against metal diffusion, providing that the PCBM layer onto which it is deposited is smooth, as explained by Boyd *et al.*[62] The deposition of a smooth PCBM layer by spin coating, for instance, leads to crack-free ITO preventing the diffusion of metallic species and the ingress of water. As mentioned in the previous paragraph, metal contacts can be substituted with TCOs or carbon based electrodes. However these materials are roughly a hundred times less conductive than metals and this severely limits the current output of the device.

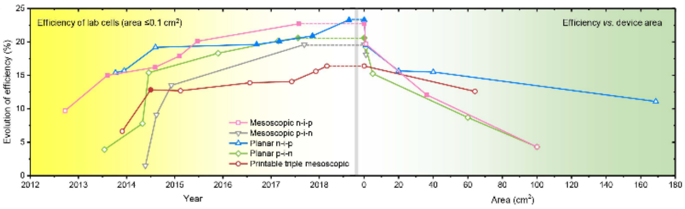

Figure 4. *Efficiency drop with area for different PSCs configurations. Reproduced from Ref*[57].

Even the inert glass substrate can play a role in the device stability. An aspect which is often ignored is the fact that perovskites have a thermal expansion coefficient (TEC) ten times larger than glass. This causes considerable residual tensile stress after spin coating and annealing as the perovskite contracts much more than the substrate upon cooling[62]. Over time, this stress can accelerate degradation of the film even at low levels of moisture (25%), whereas films placed under compressive stress did not degrade[63]. The immense advantage of flexible substrates, beyond their flexibility (a necessary requirement for roll-to-roll production), is their *low weight* compared to glass substrates, which allow one to install them much more easily on buildings façades without the need for expensive support structures or scaffolds and thus reducing the overall installation costs. Exploration of novel materials synthesis and fabrication techniques will also pave the road for easy and low temperature deposition protocols, minimizing the number of steps and making it feasible for large area production.

6. Scaling-up, measuring and reporting issues

Compared with other PV technologies such as silicon or CIGS, PSCs display a much sharper drop in PCE with the active area[57,64] (Fig. 4). Over the thousands of papers published on PSCs in the last five years, only 79 deal with "large area" concept, *i.e.* ≥ 1 cm² active area[65]. This is a critical challenge. Almost all studies are performed on cells with an active area of 0.25 mm² or less, which highlight a) the pressure to advance in the efficiency record, and b) the difficulty to obtain uniform, pinholes-free films and consistent measurements, with the result that only the best performing samples are presented whereas the poorly performing ones are disregarded. A serious statistical analysis is seldom reported. To be able to understand the behavior of PSCs and to mass produce hundreds of square metres of pinhole-free perovskite these issues must be addressed. If the research community now acknowledges peculiar characteristics of PSCs such as current-voltage hysteresis and performs measurements that account for them, stability studies still lack standardized guidelines. Tiihonen *et al.*[66] have analysed 261 papers on the subject published in 2016, and the results are appalling. 50% of the studies are based on only one cell, and 65% of them fail to meet the basic requirements for evaluating repeatability. 61% are based on unencapsulated devices, and only for one in eight cases the cell(s) are kept under load during illumination, which is the closest state to real life working conditions. Further analysis of the literature reveals that some stability tests are carried out in the dark, or in ambient conditions (whithout monitoring of temperature and humidity variations), or for a seemingly arbitrary number of hours. PSCs should in theory fall under the IEC 61646 standard, as it deals with qualification and approval of thin-film terrestrial PV modules. To pass this standard, modules must withstand, for example, 15 kWh/m^2 of UV irradiation, 200 cycles between -40 °C and +85 °C, and 1000 hours under illumination at 85 °C, with less than 20% decrease in efficiency[67,68]. Despite the clear conditions set out in the standard, several combinations of different conditions have been used for stability tests, which makes impossible to compare results and draw meaningful conclusions. The 1000 hours/85 °C requirement was calculated as follows: given that a panel should be operational for at least 25 years, and assuming 6 hours of average solar irradiation throughout the year, this is equivalent to 54,750 hours. Assuming that the degradation reaction can be described using the Arrhenius equation (7),

$$R = A\,exp\left(-\frac{E_a}{kT}\right) \tag{7}$$

where A is the pre-exponential constant, E_a is the activation energy, κ is the Boltzmann constant and T the absolute temperature, an Acceleration Factor (AF) can be defined as the ratio of R at two different temperatures, T_{use} (usually 25 °C) and T_{test} (8):

$$AF = \frac{time_{use}}{time_{test}} = exp\left(\frac{E_a}{k}\left(\frac{1}{T_{use}} - \frac{1}{T_{test}}\right)\right) \tag{8}$$

Given that most degradation mechanism in electronic components had an average activation energy of 0.8 eV, and that in the 75-125 °C range AF varied from 2.11 to 1.82 for each 10 °C interval, an average AF of 2 every 10 °C was widely accepted as a rule of thumb[69]. Based on this AF, 25 years of operation at 25 °C are equivalent to 855 hours at 85 °C, probably rounded up to 1000 hours (or obtained by lowering the activation energy to 0.6 eV). However, this approach is extremely simplistic and makes too many assumptions. First of all, perovskites are mixed ionic-electronic semiconductors and we still do not know the exact activation energy of all degradation reactions for these materials (and it is fair to assume they are different and depend on compositions). Secondly, as Reisner *et al.*[70] pointed out, depending on the reaction involved and the climate in which the panels are to operate, 1000 hours at 85 °C and 85% RH ("Damp Heat" test) may correspond to 16 years in tropical areas, but over 100 years in Central Europe. The IEC61646 tests are not, strictly speaking, *durability tests*, but merely procedures designed to find materials and manufacturing failures in a short time frame, and there is no correlation between the damp heat test for *n* number of hours and outdoor weathering for *m* number of years, which is the result of a complex interplay of heat, irradiation (visible and UV), moisture, shading, thermal cycling, mechanical stress, pollutants, and other factors[71].

To summarize, the majority of stability tests for PSCs are far too mild and the variety of conditions specified (dark, various levels of illumination, presence or absence of UV radiation, different temperatures, etc.) or lack thereof, prevents direct comparison of the results; on the other hand the IEC 61646 standard might be too harsh, and it will not yield useful information if applied to the letter and without a *quantitative* understanding of each degradation mechanism (E_a). It took three years to reach a consensus on a common set of guidelines for OPV: bearing in mind the peculiar characteristics of PSCs, the paper by Reese *et al.*[72] might be a starting point. Researchers should present stability studies on a statistically significant number of samples, include a control set, specify the environmental conditions throughout the test ("ambient" humidity and temperature can vary greatly for different countries and from day to day), the type of illumination and encapsulation, whether the samples were under load or at open circuit, etc. This calls for the need of a deep discussion in the perovskite PV community with the aim to define a consensus on guidelines to be used for perovskite stability tests, as done at the ISOS meetings.

7. Conclusions and Open Issues

This article has presented a critical and inclusive summary of gradual advances and frontiers in the field of perovskite materials and devices, showing the main challenges and near future perspectives. Development of new ways towards efficient and stable devices is indeed the next major issue which requires to be focused urgently to launch them in the market for outdoor photovoltaic applications. From what has been reported so far, stability tests at 85 °C/1 Sun illumination at maximum power point for >1000 hours can be superated only if a massive engineering and redesigning of solar cell architecture will be adopted. Ideally, this would exclude (or limit) the use of TiO_2 nanoparticles[73], methylammonium cation[12], SPIRO-OMeTAD or organic charge transport layers[74], and metal contacts[59], which represents an enormous challenge for scientists and tehcnologist working on PSCs. Development of proper encapsulant with proper sealant, with low elastic modulus to prevent the release harmful chemicals, is an important route to further explore[75]. Engineering the perovskite dimensionality has been presented as an interesting new way towards efficient and stable devices.

In the last few years, there have been key insights in the degradation mechanism of PSCs and how to tackle them; however, there are still several issues to be addressed regarding the stability of PSCs, including (but not limited to):

- How can different groups define a common testing protocols or guidelines for long term stability, which include a standardized encapsulation?
- Why is it so difficult to obtain reproducible results and more importantly over a larger area?

- Given the large difference in thermal expansion coefficient, what is the effect of residual tensile stress on accelerated testing at high (85 °C) temperature?
- Can organic charge transport layers guarantee stable performances over 25 years or is it necessary to focus more on inorganic materials?

In addition, future research directions regarding perovskite devices should also include a deeper fundamental understanding of the structural and photophysical properties of the materials under operative conditions, to realize optimum designs for stable and efficent perovskite technology.

Acknowledgements

The authors acknowledge the “HY-NANO” project that has received funding from the European Research Council (ERC) Starting Grant 2018 under the European Union’s Horizon 2020 research and innovation programme (Grant agreement No. 802862).

References

1. Kojima, A., Teshima, K., Shirai, Y. & Miyasaka, T. Organometal Halide Perovskites as Visible-Light Sensitizers for Photovoltaic Cells. *J. Am. Chem. Soc.* **131**, 6050–6051 (2009).
2. Correa-Baena, J.-P. *et al.* Promises and challenges of perovskite solar cells. *Science* **358**, 739–744 (2017).
3. Jung, H. S. & Park, N.-G. Perovskite Solar Cells: From Materials to Devices. *Small* **11**, 10–25 (2015).
4. Yang, S., Fu, W., Zhang, Z., Chen, H. & Li, C.-Z. Recent advances in perovskite solar cells: efficiency, stability and lead-free perovskite. *J. Mater. Chem. A* **5**, 11462–11482 (2017).
5. Jena, A. K., Kulkarni, A. & Miyasaka, T. Halide Perovskite Photovoltaics: Background, Status, and Future Prospects. *Chem. Rev.* **119**, 3036–3103 (2019).
6. Stranks, S. D. & Snaith, H. J. Metal-halide perovskites for photovoltaic and light-emitting devices. *Nat. Nanotechnol.* **10**, 391–402 (2015).
7. Carnie, M. J. *et al.* A one-step low temperature processing route for organolead halide perovskite solar cells. *Chem. Commun.* **49**, 7893–7895 (2013).
8. Huang, J., Tan, S., Lund, P. D. & Zhou, H. Impact of H2O on organic–inorganic hybrid perovskite solar cells. *Energy Environ. Sci.* **10**, 2284–2311 (2017).
9. Yang, J., Siempelkamp, B. D., Liu, D. & Kelly, T. L. Investigation of CH3NH3PbI3 Degradation Rates and Mechanisms in Controlled Humidity Environments Using in Situ Techniques. *ACS Nano* **9**, 1955–1963 (2015).
10. Song, Z. *et al.* Perovskite Solar Cell Stability in Humid Air: Partially Reversible Phase Transitions in the PbI2-CH3NH3I-H2O System. *Adv. Energy Mater.* **6**, 1600846 (2016).
11. Juarez-Perez, E. J. *et al.* Photodecomposition and thermal decomposition in methylammonium halide lead perovskites and inferred design principles to increase photovoltaic device stability. *J. Mater. Chem. A* **6**, 9604–9612 (2018).
12. Conings, B. *et al.* Intrinsic Thermal Instability of Methylammonium Lead Trihalide Perovskite. *Advanced Energy Materials* https://onlinelibrary.wiley.com/doi/abs/10.1002/aenm.201500477 (2015) doi:10.1002/aenm.201500477.
13. Juarez-Perez, E. J., Hawash, Z., Raga, S. R., Ono, L. K. & Qi, Y. Thermal degradation of CH3NH3PbI3 perovskite into NH and CH3I gases observed by coupled thermogravimetry–mass spectrometry analysis. *Energy Environ. Sci.* **9**, 3406–3410 (2016).
14. Latini, A., Gigli, G. & Ciccioli, A. A study on the nature of the thermal decomposition of methylammonium lead iodide perovskite, CH3NH3PbI3: an attempt to rationalise contradictory experimental results. *Sustain. Energy Fuels* **1**, 1351–1357 (2017).
15. Buin, A., Comin, R., Xu, J., Ip, A. H. & Sargent, E. H. Halide-Dependent Electronic Structure of Organolead Perovskite Materials. *Chem. Mater.* **27**, 4405–4412 (2015).
16. Li, Z. *et al.* Stabilizing Perovskite Structures by Tuning Tolerance Factor: Formation of Formamidinium and Cesium Lead Iodide Solid-State Alloys. *Chem. Mater.* **28**, 284–292 (2016).
17. Jodlowski, A. D. *et al.* Large guanidinium cation mixed with methylammonium in lead iodide perovskites for 19% efficient solar cells. *Nat. Energy* **2**, 972–979 (2017).
18. El-Mellouhi, F. *et al.* Hydrogen Bonding and Stability of Hybrid Organic–Inorganic Perovskites. *ChemSusChem* **9**, 2648–2655 (2016).

19. Eperon, G. E. *et al.* Perovskite-perovskite tandem photovoltaics with optimized band gaps. *Science* **354**, 861–865 (2016).
20. Gratia, P. *et al.* Intrinsic Halide Segregation at Nanometer Scale Determines the High Efficiency of Mixed Cation/Mixed Halide Perovskite Solar Cells. *J. Am. Chem. Soc.* **138**, 15821–15824 (2016).
21. Aristidou, N. *et al.* Fast oxygen diffusion and iodide defects mediate oxygen-induced degradation of perovskite solar cells. *Nat. Commun.* **8**, 15218 (2017).
22. Bryant, D. *et al.* Light and oxygen induced degradation limits the operational stability of methylammonium lead triiodide perovskite solar cells. *Energy Environ. Sci.* **9**, 1655–1660 (2016).
23. Pearson, A. J. *et al.* Oxygen Degradation in Mesoporous Al2O3/CH3NH3PbI3-xClx Perovskite Solar Cells: Kinetics and Mechanisms. *Adv. Energy Mater.* **6**, 1600014 (2016).
24. Lee, J.-W. *et al.* Formamidinium and Cesium Hybridization for Photo- and Moisture-Stable Perovskite Solar Cell. *Adv. Energy Mater.* **5**, 1501310 (2015).
25. Christians, J. A. *et al.* Tailored interfaces of unencapsulated perovskite solar cells for >1,000 hour operational stability. *Nat. Energy* **3**, 68–74 (2018).
26. Bu, T. *et al.* A novel quadruple-cation absorber for universal hysteresis elimination for high efficiency and stable perovskite solar cells. *Energy Environ. Sci.* **10**, 2509–2515 (2017).
27. Kubicki, D. J. *et al.* Phase Segregation in Cs-, Rb- and K-Doped Mixed-Cation (MA)x(FA)1–xPbI3 Hybrid Perovskites from Solid-State NMR. *J. Am. Chem. Soc.* **139**, 14173–14180 (2017).
28. Li, Z. *et al.* Extrinsic ion migration in perovskite solar cells. *Energy Environ. Sci.* **10**, 1234–1242 (2017).
29. Tress, W. *et al.* Understanding the rate-dependent J-V hysteresis, slow time component, and aging in CH3NH3PbI3 perovskite solar cells: the role of a compensated electric field. *Energy Environ. Sci.* **8**, 995–1004 (2015).
30. Eames, C. *et al.* Ionic transport in hybrid lead iodide perovskite solar cells. *Nat. Commun.* **6**, 7497 (2015).
31. M. Azpiroz, J., Mosconi, E., Bisquert, J. & Angelis, F. D. Defect migration in methylammonium lead iodide and its role in perovskite solar cell operation. *Energy Environ. Sci.* **8**, 2118–2127 (2015).
32. Yuan, Y. & Huang, J. Ion Migration in Organometal Trihalide Perovskite and Its Impact on Photovoltaic Efficiency and Stability. *Acc. Chem. Res.* **49**, 286–293 (2016).
33. Yuan, Y. *et al.* Photovoltaic Switching Mechanism in Lateral Structure Hybrid Perovskite Solar Cells. *Adv. Energy Mater.* **5**, 1500615 (2015).
34. Minns, J. L., Zajdel, P., Chernyshov, D., van Beek, W. & Green, M. A. Structure and interstitial iodide migration in hybrid perovskite methylammonium lead iodide. *Nat. Commun.* **8**, 15152 (2017).
35. Shao, Y., Xiao, Z., Bi, C., Yuan, Y. & Huang, J. Origin and elimination of photocurrent hysteresis by fullerene passivation in CH 3 NH 3 PbI 3 planar heterojunction solar cells. *Nat. Commun.* **5**, 1–7 (2014).
36. T. Hoke, E. *et al.* Reversible photo-induced trap formation in mixed-halide hybrid perovskites for photovoltaics. *Chem. Sci.* **6**, 613–617 (2015).
37. Unger, E. L. *et al.* Roadmap and roadblocks for the band gap tunability of metal halide perovskites. *J. Mater. Chem. A* **5**, 11401–11409 (2017).
38. Yoon, S. J., Kuno, M. & Kamat, P. V. Shift Happens. How Halide Ion Defects Influence Photoinduced Segregation in Mixed Halide Perovskites. *ACS Energy Lett.* **2**, 1507–1514 (2017).
39. Grancini, G. & Nazeeruddin, M. K. Dimensional tailoring of hybrid perovskites for photovoltaics. *Nat. Rev. Mater.* **4**, 4–22 (2019).
40. Bouduban, M. E. F. *et al.* Crystal Orientation Drives the Interface Physics at Two/Three-Dimensional Hybrid Perovskites. *J. Phys. Chem. Lett.* 5713–5720 (2019) doi:10.1021/acs.jpclett.9b02224.
41. Cho, K. T. *et al.* Water-Repellent Low-Dimensional Fluorous Perovskite as Interfacial Coating for 20% Efficient Solar Cells. *Nano Lett.* **18**, 5467–5474 (2018).
42. Grancini, G. *et al.* One-Year stable perovskite solar cells by 2D/3D interface engineering. *Nat. Commun.* **8**, 15684 (2017).
43. Jung, E. H. *et al.* Efficient, stable and scalable perovskite solar cells using poly(3-hexylthiophene). *Nature* **567**, 511–515 (2019).
44. Malinauskas, T. *et al.* Enhancing Thermal Stability and Lifetime of Solid-State Dye-Sensitized Solar Cells via Molecular Engineering of the Hole-Transporting Material

Spiro-OMeTAD. *ACS Appl. Mater. Interfaces* **7**, 11107–11116 (2015).

45. Jung, J. W., Chueh, C.-C. & Jen, A. K.-Y. A Low-Temperature, Solution-Processable, Cu-Doped Nickel Oxide Hole-Transporting Layer via the Combustion Method for High-Performance Thin-Film Perovskite Solar Cells. *Adv. Mater.* **27**, 7874–7880 (2015).
46. Liu, Z. *et al.* High-Performance Planar Perovskite Solar Cells Using Low Temperature, Solution-Combustion-Based Nickel Oxide Hole Transporting Layer with Efficiency Exceeding 20%. *Adv. Energy Mater.* **8**, 1703432 (2018).
47. Chen, W. *et al.* Cesium Doped NiOx as an Efficient Hole Extraction Layer for Inverted Planar Perovskite Solar Cells. *Adv. Energy Mater.* **7**, 1700722 (2017).
48. Yu, Z.-K. *et al.* Solution-processed CuOx as an efficient hole-extraction layer for inverted planar heterojunction perovskite solar cells. *Chin. Chem. Lett.* **28**, 13–18 (2017).
49. Zuo, C. & Ding, L. Solution-Processed Cu2O and CuO as Hole Transport Materials for Efficient Perovskite Solar Cells. *Small* **11**, 5528–5532 (2015).
50. Christians, J. A., Fung, R. C. M. & Kamat, P. V. An Inorganic Hole Conductor for Organo-Lead Halide Perovskite Solar Cells. Improved Hole Conductivity with Copper Iodide. *J. Am. Chem. Soc.* **136**, 758–764 (2014).
51. Nazari, P. *et al.* Physicochemical Interface Engineering of CuI/Cu as Advanced Potential Hole-Transporting Materials/Metal Contact Couples in Hysteresis-Free Ultralow-Cost and Large-Area Perovskite Solar Cells. *J. Phys. Chem. C* **121**, 21935–21944 (2017).
52. Arora, N. *et al.* Perovskite solar cells with CuSCN hole extraction layers yield stabilized efficiencies greater than 20%. *Science* **358**, 768–771 (2017).
53. Wijeyasinghe, N. *et al.* Copper(I) Thiocyanate (CuSCN) Hole-Transport Layers Processed from Aqueous Precursor Solutions and Their Application in Thin-Film Transistors and Highly Efficient Organic and Organometal Halide Perovskite Solar Cells. *Adv. Funct. Mater.* **27**, 1701818 (2017).
54. Li, W. *et al.* Enhanced UV-light stability of planar heterojunction perovskite solar cells with caesium bromide interface modification. *Energy Environ. Sci.* **9**, 490–498 (2016).
55. Pérez-Tomas, A. *et al.* PbZrTiO 3 ferroelectric oxide as an electron extraction material for stable halide perovskite solar cells. *Sustain. Energy Fuels* **3**, 382–389 (2019).
56. Coll, M. *et al.* Towards Oxide Electronics: a Roadmap. *Appl. Surf. Sci.* **482**, 1–93 (2019).
57. Rong, Y. *et al.* Challenges for commercializing perovskite solar cells. *Science* **361**, eaat8235 (2018).
58. Boyd, C. C., Cheacharoen, R., Leijtens, T. & McGehee, M. D. Understanding Degradation Mechanisms and Improving Stability of Perovskite Photovoltaics. *Chem. Rev.* **119**, 3418–3451 (2019).
59. Hoffmann, L. *et al.* Spatial Atmospheric Pressure Atomic Layer Deposition of Tin Oxide as an Impermeable Electron Extraction Layer for Perovskite Solar Cells with Enhanced Thermal Stability. *ACS Appl. Mater. Interfaces* **10**, 6006–6013 (2018).
60. Bush, K. A. *et al.* Thermal and Environmental Stability of Semi-Transparent Perovskite Solar Cells for Tandems Enabled by a Solution-Processed Nanoparticle Buffer Layer and Sputtered ITO Electrode. *Adv. Mater. Deerfield Beach Fla* **28**, 3937–3943 (2016).
61. Seo, S., Jeong, S., Bae, C., Park, N.-G. & Shin, H. Perovskite Solar Cells with Inorganic Electron- and Hole-Transport Layers Exhibiting Long-Term (≈500 h) Stability at 85 °C under Continuous 1 Sun Illumination in Ambient Air. *Adv. Mater.* **30**, 1801010 (2018).
62. Boyd, C. C. *et al.* Barrier Design to Prevent Metal-Induced Degradation and Improve Thermal Stability in Perovskite Solar Cells. *ACS Energy Lett.* **3**, 1772–1778 (2018).
63. Rolston, N. *et al.* Engineering Stress in Perovskite Solar Cells to Improve Stability. *Adv. Energy Mater.* **8**, 1802139 (2018).
64. Yang, M. *et al.* Square-Centimeter Solution-Processed Planar CH3NH3PbI3 Perovskite Solar Cells with Efficiency Exceeding 15%. *Adv. Mater.* **27**, 6363–6370 (2015).
65. Web of Science. *Web of Science* https://www.webofknowledge.com.
66. Tiihonen, A. *et al.* Critical analysis on the quality of stability studies of perovskite and dye solar cells. *Energy Environ. Sci.* **11**, 730–738 (2018).
67. SASO-IEC 61646/2016 Thin film terrestrial photovoltaic (PV) modules - Design qualification and type approval. *Saudi Standards, Metrology and Quality Org.*

https://www.saso.gov.sa/ar/about/PublicConsultation/Documents/SASO%20IEC%2061646-ed2%200-en.pdf.

68. Wang, D., Wright, M., Elumalai, N. K. & Uddin, A. Stability of perovskite solar cells. *Sol. Energy Mater. Sol. Cells* **147**, 255–275 (2016).
69. Wilcoxon, R. Does a 10°C Increase in Temperature Really Reduce the Life of Electronics by Half? *Electronics Cooling* https://www.electronics-cooling.com/2017/08/10c-increase-temperature-really-reduce-life-electronics-half/ (2017).
70. Reisner, E. U., Stollwerck, G., Peerlings, H. & Shafiq, F. Humidity in a Solar Module - Horror Vision or Negligible? in *Proceedings of the 21st European Photovoltaic Solar Energy Conference* 2058–2060 (2006).
71. Haillant, O. Accelerated weathering testing principles to estimate the service life of organic PV modules. *Sol. Energy Mater. Sol. Cells* **95**, 1284–1292 (2011).
72. Reese, M. O. *et al.* Consensus stability testing protocols for organic photovoltaic materials and devices. *Sol. Energy Mater. Sol. Cells* **95**, 1253–1267 (2011).
73. Leijtens, T. *et al.* Overcoming ultraviolet light instability of sensitized TiO_2 with meso-superstructured organometal tri-halide perovskite solar cells. *Nat. Commun.* **4**, 2885 (2013).
74. Chen, W. *et al.* Efficient and stable large-area perovskite solar cells with inorganic charge extraction layers. *Science* **350**, 944–948 (2015).
75. Cheacharoen, R. *et al.* Encapsulating perovskite solar cells to withstand damp heat and thermal cycling. *Sustain. Energy Fuels* **2**, 2398–2406 (2018).